analytical chemistry

pubs.acs.org/ac Article

Magneto-Mediated Electrochemical Sensor for Simultaneous Analysis of Breast Cancer Exosomal Proteins

Yu An, Rui Li, Fan Zhang,* and Pingang He

Cite This: *Anal. Chem.* 2020, 92, 5404−5410 Read Online

ACCESS | Metrics & More | Article Recommendations | Supporting Information

ABSTRACT: Breast cancer is a heterogeneous disease, and it lacks special tumor markers. Exosomes, new noninvasive biomarkers, with the proteins on the exosome surface show potential for the diagnosis and prognosis of a tumor. However, assessing the variations of exosomal proteins still faces significant challenges. Herein, a magneto-mediated electrochemical sensor based on host−guest recognition has been developed for simultaneous analysis of breast cancer exosomal proteins. Magnetic beads (MB) modified with CD63 aptamer was first employed to capture exosomes. Silica nanoparticles (SiO_2 NPs) was modified with MUC1, HER2, EpCAM, and CEA aptamers for specific exosomal proteins identification, respectively, and functionalized with *N*-(2-((2-aminoethyl)disulfanyl)ethyl) ferrocene carboxamide ($FcNHSSNH_2$) as the signal molecule. The sandwich structure (MB-exosomes-SiO_2 NPs probe) was separated by a magnet, and *N*-(2-mercaptoethyl) ferrocene carboxamide (FcNHSH) was released to the supernatant by the addition of reductants (dithiothreitol, DTT) that break the disulfide bond of $FcNHSSNH_2$. FcNHSH and the graphene oxide-cucurbit [7](GO-CB[7]) modified screen-printed carbon electrode (SPCE) was employed to monitor the oxidation current signals. In this way, four tumor markers on different breast cancer cells (MCF-7, SK-BR-3, MDA-MB-231, and BT474) derived exosomes were sensitively detected. Furthermore, the present assay enabled accurate analysis of exosomes from breast cancer patients, suggesting the potential of exosome analysis in clinic diagnosis.

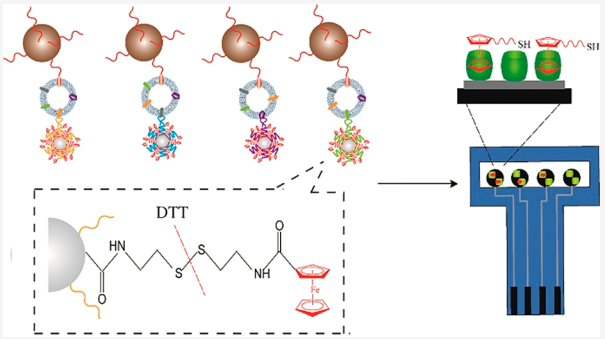

Breast cancer is one of the common malignant tumors that endangers women's healthy, and the incidence rate is increasing year by year all over the world.[1] It is a heterogeneous disease, and there are various subtypes with different clinical behaviors.[2] The protein expression level has an important diagnostic value for clinical diagnostics and classification due to the different expression in different subtypes.[3−5] Tumor markers are widely used in the diagnosis and prognosis of tumors. However, there is still a lack of specific tumor markers for breast cancer to date.[6,7] Hence, combined detection of tumor markers is of great significance for early diagnosis, clinical detection, and prognosis of breast cancer.

Exosomes are lipid bilayer membrane vesicles (30−150 nm in diameter) secreted by numerous cell types and ubiquitous in presence in saliva, serum, urine, tears, and other body fluids.[8−10] Exosomes transport various molecular contents of the cell from which they originate, including proteins and nucleic acids.[11,12] In particular, the exosomes carry a variety of tumor-specific proteins on their surfaces, which can guide various pathological and physiological processes in many signaling pathways.[13−15] Early diagnosis and treatment of breast cancer are the key to improve survival rate. Studies have shown that saliva and serum derived exosomes can be employed for the diagnosis of breast cancer.[16,17] Therefore, exosomes, as a new biomarker, can be employed for the detection of breast cancers. In particular, evaluation of exosomal surface proteins has important research implication for the diagnosis and prognosis of a tumor.[18,19] However, analyzing the subtle variations of exosomal proteins among different cell subtypes still faces significant challenges due to lack of adequately accurate and sensitive assay platforms.

Currently, there are various methods for the determination of exosomal proteins. Flow cytometry is used for the high-throughput detection of exosomes, but the vesicles with a diameter <100 nm are easy to miss, which decreases the accuracy of the measurement.[20] Mass spectrometry, enzyme-linked immunosorbent assays (ELISA), and Western blot can analyze the abundant exosomal proteins but require a large number of samples and complex procedures, limiting the application in clinical research.[21,22] Recently, fluorescence sensing[23] and nanoplasmonic sensing[24] were employed for

Received: January 9, 2020
Accepted: March 11, 2020
Published: March 11, 2020

https://dx.doi.org/10.1021/acs.analchem.0c00106
Anal. Chem. 2020, 92, 5404−5410

exosomes analysis with high sensitivity. However, the former was susceptible to photobleaching and the latter required expensive instruments. Additionally, an electrochemical platform was used for exosomal proteins profiling.[25,26] Lee et al. developed an eight-channel sensor for the simultaneous analysis of multiple exosome markers based on an integrated magneto-electrochemical assay.[26] However, it requires specialized equipment. Therefore, there is an urgent need to detection exosomal proteins in a convenient and reliable method.

In this work, an electrochemical sensor based on host−guest recognition was developed for the simultaneous determination of tumor exosomal proteins (Scheme 1). Mucin 1 (MUC1)

Scheme 1. Schematic Representation of the Magneto-Mediated Electrochemical Sensor for Exosomal Proteins Analysis Based on Host−Guest Recognition

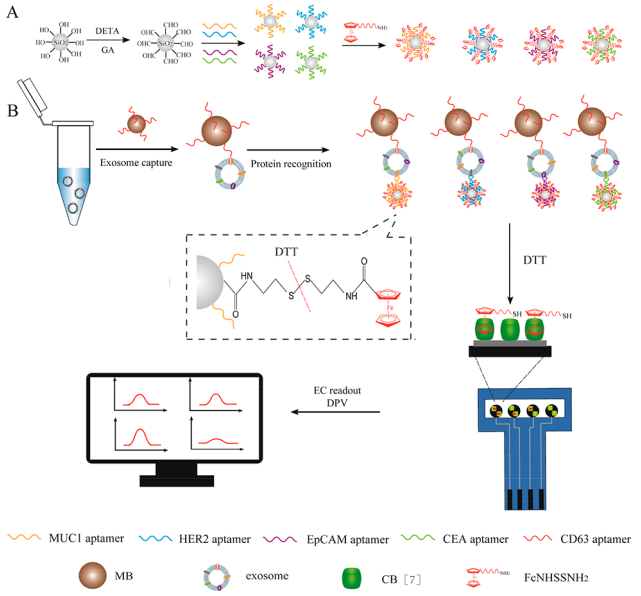

protein is a high molecular weight glycoprotein, which is highly and abnormally expressed in breast cancer.[27] Human epidermal growth factor receptor-2 (HER2) overexpression can increase the invasive and metastasis ability of tumor cancer and is an important predictor and prognostic marker for breast cancer.[28] Epithelial cell adhesion molecule (EpCAM) is highly expressed in almost all adenocarcinomas and affects the occurrence of epithelial-mesenchymal transformation of breast cancer cells.[29] Carcino-embryonic antigen (CEA) is highly specific and sensitive for the detection of breast cancer, which is one of the independent prognostic indicators of breast cancer.[30] Hence, MUC1, HER2, EpCAM, and CEA proteins were employed for combined detection of breast cancer in this work. CD63 is a member of four transmembrane protein superfamily and is widely and highly expressed on the surface of many breast cancer exosome types.[31−33] Therefore, CD63 aptamers were modified on the magnetic beads (MB) for tumor exosomes capture. The silica nanoparticles (SiO_2 NPs) were modified with MUC1, HER2, EpCAM, and CEA aptamers for specific exosomal proteins identification, respectively. Then, $FcNHSSNH_2$, which has multiple functional groups, including amino groups, disulfide bond, and ferrocene, was combined with SiO_2 NPs by the reaction of the amino group and the aldehyde group and used as a signal molecule. When exosomes were present, the MB probe and SiO_2 NPs probe formed the sandwich structure, which was separated from unbound SiO_2 NPs probes by a magnet and FcNHSH was released to the supernatant by the addition of reductants (dithiothreitol, DTT) that break the disulfide bond of $FcNHSSNH_2$. Subsequently, the graphene oxide-cucurbit[7] (GO-CB[7]) modified screen-printed carbon electrode (SPCE) could form stable complexes with FcNHSH through host−guest interaction, which effectively avoided the modification of exosomes onto the electrode. Exosomal proteins were further quantified by the oxidation current signal of FcNHSH. In this way, four tumor markers on the surface of exosomes from different breast cancers (MCF-7, SK-BR-3, MDA-MB-231, and BT474) were accurately and sensitively detected, which has potential application in early diagnosis, clinical detection, and prognosis of breast cancer.

EXPERIMENTAL SECTION

Reagents and Materials. All oligonucleotides were synthesized by the Sangon Biological Engineering Technology & Services Co., Ltd. (Shanghai, China) and listed in Table S1. Ferrocenecarboxylic acid, *N*-hydroxysuccinimide and cystaminedihydrochloride were purchased from Sigma-Aldrich (St. Louis, MO). Cyclohexane, 1-hexanol, triton X-100, and silicon tetraacetate (TEOS) were purchased from the Sinopharm Chemical Reagent Co. (Shanghai, China). Graphite oxide was obtained from the Jcnano Chemical Industry Co., Ltd. (Nanjing, China). Dithiothreitol (DTT), trimethoxysilylpropyldiethylenetriamine (DETA), and cucurbituril (CB[7]) were purchased from Sigma-Aldrich (St. Louis, MO). Rabbit antihuman MUC1 polyclonal antibody, rabbit antihuman HER2 polyclonal antibody, rabbit antihuman EpCAM polyclonal antibody, rabbit antihuman CEA polyclonal antibody, and HRP conjugated rabbit polyclonal secondary antibody were purchased from Abcam Pic. (Cambridge, U.K.). The bicinchoninic acid (BCA) protein assay kit and radio-immunoprecipitation assay (RIPA) lysis buffer were obtained from the Beyotime Biotechnology Co. Ltd. (Shanghai, China). Dulbecco's modified eagle medium (DMEM), Roswell Park Memorial Institute (RPMI) 1640 medium, fetal bovine serum (FBS), trypsin/EDTA solution, penicillin/streptomycin (P/S), and Dulbecco's phosphate buffered saline (PBS) were obtained from Thermo Fisher Scientific Inc. (Waltham, MA). Exosome-depleted fetal bovine serum and the ExoQuickExosome Isolation Kit were purchased from System Biosciences Inc. (SBI). The human breast cancer cell line (MCF-7, SK-BR-3, MDA-MB-231, and BT474) were obtained from the Chinese Academy of Sciences (Shanghai, China). The filters (0.22 μm in aperture) were purchased from theMillipore Corp. (Bedford, MA).

A Tris-HCl buffer (5 mM, pH = 7.5) containing 0.5 mM EDTA and 1 M NaCl was used as the washing buffer. A phosphate buffered saline (PBS, 10 mM, pH = 7.4) containing 0.1 M KCl was employed as the electrochemical detection solution. All solutions were prepared with deionized water (DI, $\geq$18.2 MΩ cm^{-1}) by a Milli-Q water purification system (Millipore Corp., Bedford, MA).

Instrumentation. MCF-7, SK-BR-3, MDA-MB-231, and BT474 cells were cultured in a humidified incubator (NuAire). The transmission electron microscopy (TEM) characterization of exosomes and SiO_2 NPs were performed on a Hitachi-7700 instrument (Tokyo, Japan) and JEOL JEM-2100 (Hitachi, Japan), respectively. Zeta potential characterization were

https://dx.doi.org/10.1021/acs.analchem.0c00106
Anal. Chem. 2020, 92, 5404−5410

performed on a ZetasizerNano (Malvern, England). ^{1}H NMR and ^{13}C NMR were performed using an AVANCEIII 500 (Bruker, Germany). Sodium dodecyl sulfate-polyacrylamide gel electrophoresis (SDS-PAGE) was performed on a BioRad electrophoresis apparatus and imaged on a Typhoon 9410 variable mode imager (Amersham). Electrochemical measurements were carried out on a CHI1030C electrochemical workstation (Chenhua, Shanghai, China).

Preparation of $FcNHSSNH_2$. Cystaminedihydrochloride (2.55 g, 11.33 mM) was first suspended in 50 mL of $CHCl_3$ and then treated with an aqueous solution of NaOH (2 M, 50 mL). The aqueous phase was extracted three times with $CHCl_3$. The combined organic phase was dried overnight with anhydrous $MgSO_4$. The solvent was removed by rotary evaporation to yield cystamine.[34] Ferrocene carboxylic acid (1.03 g, 4.5 mM) was dissolved in 70 mL of anhydrous CH_2Cl_2. Then, *N*-hydroxysuccinimide (0.61 mg, 5.3 mM) and *N*-(3-(dimethylamino)propyl)-*N*′-ethycarbodiimide hydrochloride (0.98 mg, 5.2 mM) were added, and the reaction mixture was stirred overnight at room temperature. After the solution was washed three times with water, the combined water phases were extracted with CH_2Cl_2 and the combined organic phases were dried overnight with anhydrous $MgSO_4$. The solvent was removed in vacuo, and the reaction mixture was purified by silica gel chromatography (diethyl ether) to yield ferrocene-carboxylic acid *N*-succinimide ester (FcNHS).[35] The obtained FcNHS (1.56 g, 4.77 mM) was then dissolved in 50 mL of CH_2Cl_2, followed by the treatment of cystamine (1.21 g, 7.96 mM) and Et_3N (2 mL) under stirring for 12 h at room temperature. After the reaction mixture was washed three times with water, the organic phases were dried over $MgSO_4$. The solvent was removed in vacuo, and the reaction mixture was purified by silica gel chromatography (CH_2Cl_2−MeOH = 9:1) to give *N*-(2-((2-aminoethyl)disulfanyl)ethyl) ferrocene carboxamide ($FcNHSSNH_2$) as a yellow solid.[34]

Cell Culture and Exosome Isolation. The MCF-7 cells and MDA-MB-231 cells were cultured in DMEM medium containing 10% FBS and 1% P/S in a humidified incubator of 5% CO_2 and 95% air at 37 °C. The SK-BR-3 cells and BT474 cells were cultured in 1640 medium containing 10% FBS and 1% P/S. All cells reaching 80% confluence were detached with 0.25% trypsin/EDTA and centrifugated (800 rpm, 5 min) to allow for subculturing. Exosomes were isolated as reported previously.[36] In brief, the exosome-depleted FBS medium from 1×10^6 cells were collected after 48 h. Then, the medium was centrifuged successively at 300*g* for 10 min to eliminate apoptotic cells, 2000*g* for 20 min, and 10 000*g* for 30 min at 4 °C to remove the cell debris. Finally, it was filtered through a 0.22 μm filter. Afterward, the supernatant was further centrifuged at 100 000*g* for 1 h at 4 °C to collect the exosomes, followed by washing with PBS and another ultracentrifugation. Finally, the exosomes were resuspended in 100 μL of 0.01 M PBS and stored at −80 °C.

Characterization of Exosomes. The TEM characterization of exosomes from MCF-7 cells were carried out according to previous protocol.[10,37] Briefly, 5 μL of exosomes in PBS were dropped on the carbon-coated copper grid for 20 min, and then the remaining solution was evaporated in a dry environment. The pellets were further carried out via negative staining using 1% phosphotungstic acid for 10 s. The remaining solution was absorbed by filter paper and imaged using TEM.

Western blot was employed for the analysis of exosomal proteins according to previously described with modification.[10,38] The exosomes of MCF-7 cells, SK-BR-3 cells, MDA-MB-231 cells, and BT474 cells were lysed with RIPA buffer, respectively. Then, the BCA method was used for the quantification of the exosomal protein concentration. The protein samples (10 μg) was subjected to 10% SDS-PAGE and further electrotransferred to a nitrocellulose filter membrane.[10] Afterward, the membranes were blocked with 5% BSA and incubated overnight at 4 °C with the following monoclonal antibodies: α-MUC1, α-HER2, α-EpCAM, and α-CEA. Next, the blots were incubated for 1 h with HRP-conjugated rabbit polyclonal antibodies and the protein strips was imaged by a Gel Image System.

Preparation of Magnetic Beads (MB) Probe. The preparation of aptamers-modified magnetic beads was carried out as reported previously.[39] Briefly, 12.5 μL of streptavidin-modified magnetic beads (10 mg/mL) were first washed three times with 5 mM Tris-HCl buffer (pH 7.5) containing 0.5 mM EDTA and 1 M NaCl and resuspended in 50 μL of 0.1 M PBS (pH 7.4) containing 0.1 M KCl. Then, 3 μL of 100 μM biotin-CD63 aptamer was added to the above solution with gentle shaking at 37 °C for 2 h, followed by washing three times with 0.1 M PBS. Next, the pellets were resuspended in 50 μL of 0.01 M PBS.

Preparation of SiO_2 NPs Probes. First, the SiO_2 nanoparticles (SiO_2 NPs) were prepared as the previous work.[40] Briefly, 30 mL of cyclohexane, 7.2 mL of *n*-hexanol, and 7.2 mL of Triton X-100 were stirred for 5 min. Then, 1.2 mL of ultrapure water was added to the solution, and the mixture was stirred for 30 min at room temperature. Subsequently, 400 μL of TEOS and 240 μL of $NH_3{\cdot}H_2O$ (25 wt %) were slowly dripped into the mixture and vigorously stirred for 24 h at room temperature. The defined amount of ethanol was added to the reaction mixture to break up the microemulsion, and the solution was centrifuged and washed three times with ethanol and water, respectively. The SiO_2 NPs were finally resuspended in 10 mL of ultrapure water and stored at 4 °C for further use. Afterward, 100 μL of SiO_2 NPs were aminated in 5 mL of aqueous solution containing 5% DETA and 1 mM HAc with shaking at 37 °C for 1 h.[41] The solution was centrifuged and washed three times with water. After that, the SiO_2 NPs pellets were added to 5 mL of 5% glutaraldehyde for 1 h with gentle shaking at 37 °C. Subsequently, the solution was centrifuged and washed three times with water and then was resuspended in 100 μL of 0.1 M PBS buffer. A volume of 5 μL of 100 μM amino-modified aptamer was added into the SiO_2 NPs solution with shaking for 2 h at 37 °C. Next, 1 μL of 100 mM $FcNHSSNH_2$ was added into the mixture and allowed to react for 2 h at 37 °C with gently shaking. The mixture was then washed three times with 0.1 M PBS and resuspended in 50 μL of 0.01 M PBS buffer.

Electrochemical Detection. The SPCE (3 mm in diameter) with four channels was first washed with water. Then, 7 μL of uniform GO-CB[7] suspension droplets was dropped to the SPCE and dried at room temperature.[42] The procedures for exosomes detection was as follows. First, 50 μL of MB probe was incubated with exosomes under gentle shaking at 37 °C for 3 h, followed by washing with 0.01 M PBS. Then, 50 μL of SiO_2 NPs probes were added to the MB probe. After incubation for 3 h with gentle shaking, the complexes were washed with 0.01 M PBS three times. Next, 50 μL of 10 mM DTT solution was added and incubated with the

https://dx.doi.org/10.1021/acs.analchem.0c00106
Anal. Chem. 2020, 92, 5404−5410

above complexes for 30 min to break the disulfide bond.[43] Afterward, 7 μL of the supernatant solution was dropped on the GO-CB[7] modified SPCE for host−guest recognition at 37 °C. The modified SPCE was rinsed and DPV measurements were determined in 0.1 M PBS. In the three-electrode system, SPCE, Ag/AgCl electrode, and platinum wire were employed as the working electrode, the reference electrode, and the auxiliary electrode, respectively. The DPV signals were detected from 0.2 to 0.8 V with the pulse amplitude of 50 mV, pulse width of 50 ms, and pulse period of 0.2 s.

Detection of Exosomes in Human Serum. Shanghai Ruijin Hospital provided us with serum samples from breast cancer patients and healthy individuals. Exosomes from serum samples were isolated by ExoQuickExosome Isolation Kit according to previous protocol.[10] The human serum was centrifuged successively at 3 000*g* for 15 min, which could eliminate the cell debris. The supernatant was further collected in a new tube and the isolation reagent was added at the ratio of 1:4. The samples were incubated for 1 h at 4 °C and centrifugated at 1 500*g* for 30 min to obtain exosome pellets. Then, the exosome pellets were resuspended in 500 μL of 0.01 M PBS solution and stored at −80 °C. The electrochemical measurement procedures were consistent with those for the exosomes detection described above.

RESULTS AND DISCUSSION

Feasibility of this Strategy. The morphology of MCF-7 exosomes was observed on the TEM image. As shown in Figure 1A, these exosomes presented a typical cup shape

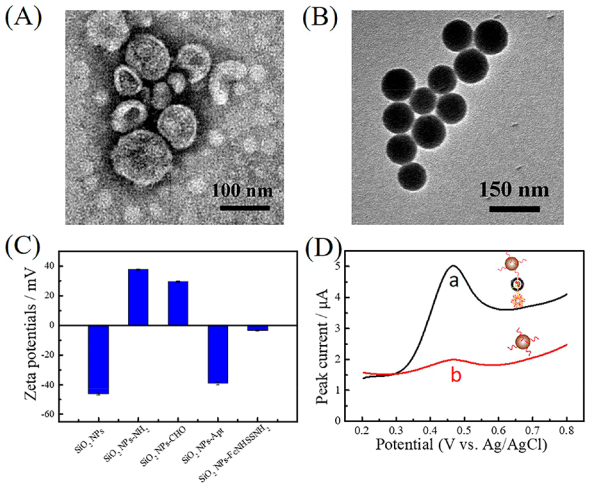

Figure 1. (A) TEM image of the MCF-7 exosomes; (B) TEM image of SiO_2 NPs; (C) zeta potential of the SiO_2 NPs probe; (D) DPV signals with (a) and without (b) the MCF-7 exosomes at concentration of 1.2×10^6 particles/μL.

morphology. Meanwhile, these exosomes contained double-walled lipid membrane layers at a diameter of 50−100 nm, consistent with reported exosomes.[10,37] Meanwhile, nanoparticle tracking analysis (NTA) was used to characterize the concentration of all isolated exosomes. To confirm the modification of SiO_2 NPs probe, TEM and zeta potential were employed. As shown in Figure 1B, SiO_2 NPs have a smooth spherical structure with a diameter of ∼100 nm as well as good dispersion. Figure 1C exhibits the surface charge change with the ammoniation of SiO_2 NPs by DETA (zeta potential, −46.3 mV) to obtain SiO_2 NPs-NH_2 (zeta potential, 37.5 mV). After the surface modification of glutaraldehyde, the zeta potential decreases to 29.5 mV, indicating the successful functionalization of aldehyde group, obtaining SiO_2 NPs-CHO.[44,45] When the aptamers with negative charges were coupled to the nanoparticles (SiO_2 NPs-Apt), the zeta potential was dramatically reduced to −39.0 mV. While the zeta potential is increased to −3.36 mV, the $FcNHSSNH_2$ molecule was modified on the nanoparticles to generate SiO_2 NPs-$FcNHSSNH_2$. These results prove the successful surface modification of SiO_2 NPs probe. Using the MUC1 marker on the MCF-7 exosomes as the model, the DPV responses were determined with and without the exosomes as exhibited in Figure 1D. Clearly, when the exosomes were present in the system at a concentration of 1.2×10^6 particles/μL, the current signal with exosomes was about 7 times that without exosomes. These results show that the magneto-mediated electrochemical sensor could be used for the detection of exosome markers.

Figure S1 displayed the ^1H NMR and ^{13}C NMR of FcNHS and $FcNHSSNH_2$, respectively. ^1H NMR of FcNHS (500 M Hz, $CDCl_3$) δ/ppm 4.96 (t, J = 1.9 Hz, 2 H), 4.73 (t, J = 2.0 Hz, 2 H), 4.43 (s, 5 H), 2.99−2.74 (m, 4 H); ^{13}C NMR of $FcNHSSNH_2$ (126 M Hz, $CDCl_3$) δ/ppm 169.57, 167.40, 72.83, 70.79, 70.74, 64.27, 25.67. ^1H NMR of $FcNHSSNH_2$ (500 M Hz, DMSO-d_6) δ/ppm 7.98 (s, 1 H), 4.78 (t, J = 1.9 Hz, 2 H), 4.35 (t, J = 1.9 Hz, 2 H), 4.18 (s, 5 H), 3.51−3.42 (m, 2 H), 2.89 (t, J = 6.9 Hz, 2 H), 2.84 (dd, J = 7.2 Hz, 4.9 Hz, 2 H), 2.78 (dd, J = 7.2 Hz, 4.9 Hz, 2 H); ^{13}C NMR of $FcNHSSNH_2$ (126 M Hz, DMSO-d_6) δ/ppm 169.58, 76.86, 70.41, 69.85, 68.61, 42.00, 41.27, 38.77, 37.92.

Optimization of Detection Conditions. Taking the determination of MUC1 marker on MCF-7 exosomes as the model, the main experimental conditions were optimized to improve the sensitivity of the detection. Figure 2A shows the effect of the ratio between MUC1 aptamer and $FcNHSSNH_2$ on the electrochemical response. It could be observed that the current signal reaches a maximum when the ratio of MUC1 aptamer and $FcNHSSNH_2$ was 1:200. However, by increasing the ratio from 1:200 to 1:100, the current response gradually

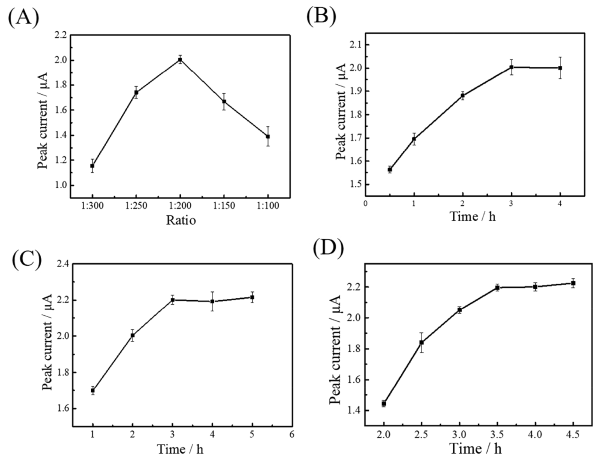

Figure 2. Effects of (A) the ratio between MUC1 aptamer and $FcNHSSNH_2$ in the MB probe, (B) incubation time of MB probe with exosomes, (C) incubation time of SiO_2 NPs probe with exosomes, and (D) recognition time of FcNHSH by GO-CB[7] with 1.12×10^6 particles/μL MCF-7 exosomes. Each data point is the mean of three measurements, and the relative standard deviation (RSD) is less than 6.3%.

https://dx.doi.org/10.1021/acs.analchem.0c00106
Anal. Chem. 2020, 92, 5404−5410

decreases, probably due to the reduction $FcNHSSNH_2$ on SiO_2 NPs. Thus, the optimal ratio was 1:200. Figure 2B exhibits that DPV responses with increasing the incubation time of exosomes with the MB probe from 0.5 to 4 h. Clearly, beyond 3 h, the current signal remains almost constant. Hence, the optimal incubation time of MB probe and exosome was 3 h. The reaction time of SiO_2 NPs probe with exosomes is another key factor for the amount of MUC1 aptamer combined with exosomes. As shown in Figure 2C, it could be observed that the current response first increases as the incubation time increases from 1 to 3 h and then remains nearly constant in the range of 3−5 h. Thus, 3 h was selected as the optimal incubating time of SiO_2 NPs probe with exosomes. Figure 2D illustrates the influence of the incubation time of FcNHSH with GO-CB[7] modified SPCE. The reduction peak current continuously increases in the range from 2.0 to 3.5 h. However, the current signal no longer changed with further extension of incubation time, suggesting that the host−guest recognition of the FcNHSH molecule with GO-CB[7] reaches saturation at 3.5 h.

Profiling of Protein Markers in Breast Cancer Cell-Derived Exosomes. Under the optimal detection conditions, the subtle changes of the MUC1 marker level in different breast cancer cells-derived exosomes were determined at various concentrations. From Figure 3A, it could be observed

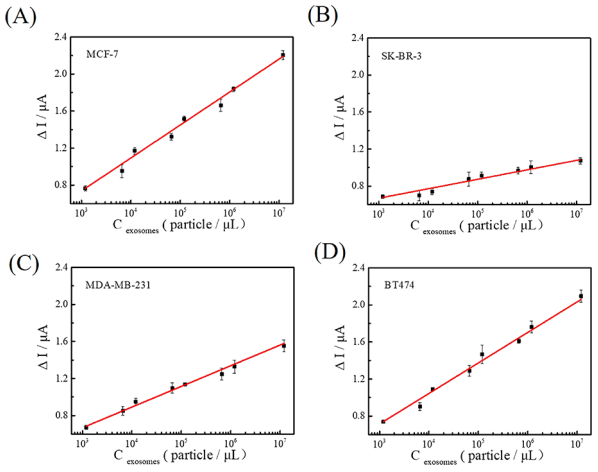

Figure 3. Analysis of MUC1 marker on (A) MCF-7, (B) SK-BR-3, (C) MDA-MB-231, and (D) BT474 cells-derived exosomes at different concentrations (1.2×10^3, 6.6×10^3, 1.2×10^4, 6.6×10^4, 1.2×10^5, 6.6×10^5, 1.2×10^6, and 1.2×10^7 particles/μL). Each data point is the mean of three measurements, and the relative standard deviation (RSD) is less than 6.3%.

that there is a linear relationship between current and the logarithm of MCF-7 cells-derived exosomes concentration in the range of 1.2×10^3 to 1.2×10^7 particles/μL. The equation is as follows: $\Delta I = 0.3561 \times \lg c - 0.3305$ ($R^2 = 0.9911$), where ΔI is the difference of current signal with and without the exosomes, and c represents the concentration of exosomes. Figure 3B presents the linear relationship between current and the logarithm of the SK-BR-3 cells-derived exosomes concentration with the equation of $\Delta I = 0.1022 \times \lg c + 0.3624$ ($R^2 = 0.9674$), The logarithm of the MDA-MB-231 cells-derived exosomes concentration in the same range and the current response have the following linear relationship: $\Delta I = 0.2232 \times \lg c - 0.0007$ ($R^2 = 0.9920$). For BT474 cells, the logarithm of exosome concentrations and the current signals satisfy a linear relationship with the equation of $\Delta I = 0.3295 \times \lg c - 0.2733$ ($R^2 = 0.9938$, Figure 3D). Clearly, the response slopes are significantly different for these four kinds of breast cancer cells-derived exosomes, suggesting the different expression level of MUC1 on exosomes: MCF-7 cells-derived exosomes present the most abundant MUC1, then BT474 cells-derived exosomes, MDA-MB-231 cells-derived exosomes, and finally SK-BR-3 cells-derived exosomes. Thus, this developed sensor could be able to distinguish the subtle changes of MUC1 level in different exosomes and might allow identification of other tumor markers.

Furthermore, the expression of four tumor markers on these breast cancer cells-derived exosomes were profiled. Figure 4A

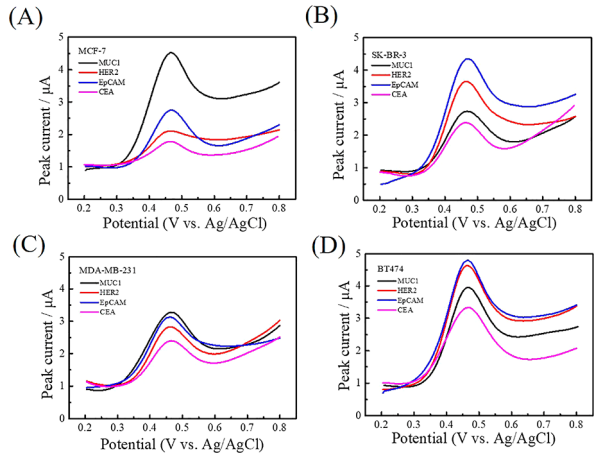

Figure 4. DPV responses of the magneto-mediated electrochemical sensor for MUC1, HER2, EpCAM, and CEA markers for the (A) MCF-7, (B) SK-BR-3, (C) MDA-MB-231, and (D) BT474 cells-derived exosomes at a concentration of 1.2×10^6 particles/μL.

presents the difference in the expression of MUC1, HER2, EpCAM, and CEA proteins on MCF-7 exosomes at a concentration of 1.2×10^6 particles/μL. Clearly, MUC1 protein is highly expressed, followed successively by EpCAM, HER2, and CEA. The same order of protein expression appears on MDA-MB-231 exosomes, while with different quantities (Figure 4C). For SK-BR-3 exosomes (Figure 4B) and BT474 exosomes (Figure 4D), the amount of EpCAM, HER2, MUC1, and CEA proteins they carry both decrease successively, but the determined values are obviously different. These results suggest that this electrochemical sensor can be employed to the distinguish the subtle changes of various tumor markers on different exosomes.

The DPV current responses of various tumor markers were summarized and presented as a heat map in Figure 5A. Meanwhile, Western blot (WB) as a traditional protein detection method was employed for comparison (Figure 5B). Clearly, the high expression of MUC1 protein is presented on MCF-7 and BT474 exosomes, compared with the moderate level on MDA-MB-231 exosomes and the minimum level on SK-BR-3 exosomes. HER2 protein is highly expressed on BT474 exosomes, followed by SK-BR-3, MDA-MB-231, and MCF-7 exosomes. For EpCAM protein, its expression level on MCF-7, SK-BR-3, MDA-MB-231, and BT474 exosomes is successively increased. CEA protein is expressed at a relatively low level except on BT474 exosomes. The results indicate that the expression levels of the tumor markers were significantly different and related to the breast cancer cells-derived

https://dx.doi.org/10.1021/acs.analchem.0c00106
Anal. Chem. 2020, 92, 5404−5410

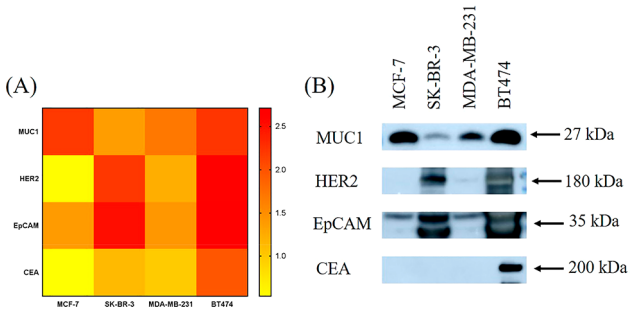

Figure 5. (A) Electrochemical responses represented as a heat map highlighting the difference of four tumor markers on four types of breast cancer cells-derived exosomes and (B) corresponding results of Western blot analysis.

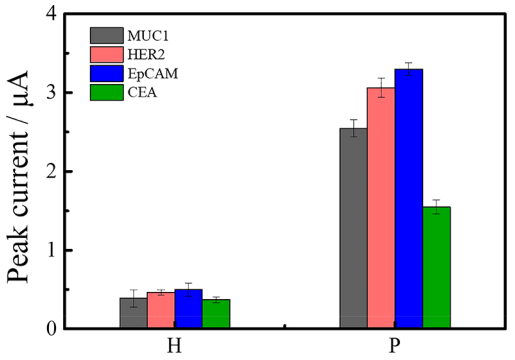

Figure 6. Detection of exosomal tumor markers in human serum with breast cancer (patient, P) and noncancer (healthy, H). Each data point is the mean of three measurements and the relative standard deviation (RSD) is less than 6.3%.

exosomes types. The obtained protein information was basically consistent with the result of WB. Our method required less exosomes sample than WB and had a higher sensitivity. Hence, the sensor can be used to classify different subtypes of breast cancer cells and allows noninvasive early diagnosis of breast cancer by combined detection of tumor markers. Moreover, compared with the reported methods (Table S2), our method presents a comparable sensitivity and wider detection linear range. More importantly, it has achieved a combined detection of exosomal proteins for breast cancer, which could improve the accuracy of detection and thus shows a high potential in early diagnosis, clinical detection, and prognosis of breast cancer.

Reproducibility and Stability of the Sensor. Taking the determination of MUC1 marker on MCF-7 cells-derived exosomes as the model, the reproducibility and stability of the electrochemical sensors were evaluated. Nine electrodes modified under the same conditions were measured, and the relative standard deviation (RSD) of current for 1.2×10^6 particles/μL exosomes was found as 6.23%, reflecting a good reproducibility of the electrochemical sensor (Figure S2A). To investigate the stability, the modified electrodes were stored at 4 °C and measured every 7 days (Figure S2B). The sensor retained almost 97.7% of the initial signal for 7 days. Fourteen days later, the current decreased to 95.9%. It had 94.8% and 90.8% of the initial values for 21 days and 28 days, respectively, presenting an excellent stability of the sensor.

Determination of Exosomes in Serum from Breast Cancer Patients. To demonstrate the practical ability of this sensor, the exosomes at a concentration of 1.0×10^7 particles/μL derived from human serum samples with breast cancer (patient, P) and noncancer (healthy, H) were analyzed. By comparing the current responses, it could be found that the expression levels of MUCI, HER2, EpCAM, and CEA proteins on breast cancer patient-derived exosomes were all higher than those on healthy individual-derived exosomes (Figure 6). The results clearly suggested that our method is suitable for analyzing the exosomes in clinical samples.

CONCLUSIONS

In summary, a magneto-mediated electrochemical sensor has been developed to profile protein markers information in breast cancer cell-derived exosomes. It employed the aptamers for the specific recognition of four exosomal proteins and took advantage of the SPCE for the simultaneous detection based on host–guest recognition between GO-CB[7] and FcNHSH. This sensor could differentiate the subtle variations of exosomal proteins among different breast cell subtypes. Meanwhile, the developed biosensor displayed great potential in the determination of exosomes in serum from breast cancer patients with high accuracy and easy operation, which is promising for clinical diagnosis.

ASSOCIATED CONTENT

Supporting Information

The Supporting Information is available free of charge at https://pubs.acs.org/doi/10.1021/acs.analchem.0c00106.

Sequences of the oligonucleotides; NMR characterization of FcNHS and $FcNHSSNH_2$; and reproducibility and stability (PDF)

AUTHOR INFORMATION

Corresponding Author

Fan Zhang − *School of Chemistry and Molecular Engineering, East China Normal University, Shanghai 200241, P. R. China;* orcid.org/0000-0003-4229-3916; Email: fzhang@chem.ecnu.edu.cn; Fax: +86-21-54340049

Authors

Yu An − *School of Chemistry and Molecular Engineering, East China Normal University, Shanghai 200241, P. R. China*

Rui Li − *School of Chemistry and Molecular Engineering, East China Normal University, Shanghai 200241, P. R. China*

Pingang He − *School of Chemistry and Molecular Engineering, East China Normal University, Shanghai 200241, P. R. China*

Complete contact information is available at: https://pubs.acs.org/10.1021/acs.analchem.0c00106

Notes

The authors declare no competing financial interest.

ACKNOWLEDGMENTS

This work was financially supported by the National Natural Science Foundation of China (Grant No. 21575042).

REFERENCES

(1) Ezzati, M.; Yousefi, B.; Velaei, K.; Safa, A. *Life Sci.* **2020**, *248*, 117463.

(2) Bianchini, G.; Balko, J. M.; Mayer, I. A.; Sanders, M. E.; Gianni, L. *Nat. Rev. Clin. Oncol.* **2016**, *13* (11), 674.

(3) Bergamaschi, A.; Kim, Y. H.; Wang, P.; Sørlie, T.; Hernandez-Boussard, T.; Lonning, P. E.; Tibshirani, R.; Børresen-Dale, A.-L.; Pollack, J. R. *Genes, Chromosomes Cancer* **2006**, *45* (11), 1033−1040.
(4) Perez-Pinera, P.; Chang, Y.; Astudillo, A.; Mortimer, J.; Deuel, T. F. *Biochem. Biophys. Res. Commun.* **2007**, *358* (2), 399−403.
(5) Kennecke, H.; Yerushalmi, R.; Woods, R.; Cheang, M. C. U.; Voduc, D.; Speers, C. H.; Nielsen, T. O.; Gelmon, K. *J. Clin. Oncol.* **2010**, *28* (20), 3271−3277.
(6) Molina, R.; Barak, V.; van Dalen, A.; Duffy, M. J.; Einarsson, R.; Gion, M.; Goike, H.; Lamerz, R.; Nap, M.; Sölétormos, M.; Stieber, P. *Tumor Biol.* **2005**, *26* (6), 281−293.
(7) Duffy, M. J. *Clin. Chem.* **2005**, *51* (3), 494−503.
(8) Ko, J.; Carpenter, E.; Issadore, D. *Analyst* **2016**, *141*, 450−460.
(9) Conlan, R. S.; Pisano, S.; Oliveira, M. I.; Ferrari, M.; Mendes Pinto, I. *Trends Mol. Med.* **2017**, *23* (7), 636−650.
(10) An, Y.; Jin, T.; Zhu, Y.; Zhang, F.; He, P. *Biosens. Bioelectron.* **2019**, *142*, 111503.
(11) Lapping-Carr, G.; Khalyfa, A.; Rangel, S.; Darlington, W.; Beyer, E. C.; Peddinti, R.; Cunningham, J. M.; Gozal, D. *Pediatr. Pulm.* **2017**, *52* (11), 1478−1485.
(12) Wang, X.; Kaczor-Urbanowicz, K. E.; Wong, D. T. W. *Med. Oncol.* **2017**, *34*, 7.
(13) Kalluri, R.; LeBleu, V. S. *Science* **2020**, *367* (6478), eaau6977.
(14) Simons, M.; Raposo, G. *Curr. Opin. Cell Biol.* **2009**, *21* (4), 575−581.
(15) Schorey, J. S.; Bhatnagar, S. *Traffic* **2008**, *9* (6), 871−881.
(16) Yu, D.; Wu, Y.; Shen, H.; Lv, M.; Chen, W.; Zhang, X.; Zhong, S.; Tang, J.; Zhao, J. *Cancer. Sci.* **2015**, *106* (8), 959−964.
(17) Friel, A. M.; Corcoran, C.; Crown, J.; O'Driscoll, L. *Breast Cancer Res. Treat.* **2010**, *123* (3), 613−625.
(18) Menck, K.; Bleckmann, A.; Wachter, A.; Hennies, B.; Ries, L.; Schulz, M.; Balkenhol, M.; Pukrop, T.; Schatlo, B.; Rost, U.; Wenzel, D.; Klemm, F.; Binder, C. *J. Extracell. Vesicles* **2017**, *6* (1), 1340745.
(19) Ohno, S.; Takanashi, M.; Sudo, K.; Ueda, S.; Ishikawa, A.; Matsuyama, N.; Fujita, K.; Mizutani, T.; Ohgi, T.; Ochiya, T.; Gotoh, N.; Kuroda, M. *Mol. Ther.* **2013**, *21* (1), 185−191.
(20) Pospichalova, V.; Svoboda, J.; Dave, Z.; Kotrbova, A.; Kaiser, K.; Klemova, D.; Ilkovics, L.; Hampl, A.; Crha, I.; Jandakova, E.; Minar, L.; Weinberger, V.; Bryja, V. *J. Extracell. Vesicles* **2015**, *4*, 25530.
(21) Nguyen, H. Q.; Lee, D.; Kim, Y.; Paek, M.; Kim, M.; Jang, K.; Oh, J.; Lee, Y.; Yeon, J. E.; Lubman, D. M.; Kim, J. *Anal. Chem.* **2019**, *91* (20), 13297−13305.
(22) Xia, Y.; Chen, T.; Chen, G.; Weng, Y.; Zeng, L.; Liao, Y.; Chen, W.; Lan, J.; Zhang, J.; Chen, J. *Talanta* **2020**, *214*, 120851.
(23) Wang, L.; Pan, Y.; Liu, Y.; Sun, Z.; Huang, Y.; Li, J.; Yang, J.; Xiang, Y.; Li, G. *ACS Appl. Mater. Interfaces* **2020**, *12*, 322−329.
(24) Im, H.; Shao, H.; Park, Y. I.; Peterson, V. M.; Castro, C. M.; Weissleder, R.; Lee, H. *Nat. Biotechnol.* **2014**, *32*, 490−495.
(25) Zhou, Y. G.; Mohamadi, R. M.; Poudineh, M.; Kermanshah, L.; Ahmed, S.; Safaei, T. S.; Stojcic, J.; Nam, R. K.; Sargent, E. H.; Kelley, S. O. *Small* **2016**, *12* (6), 727−732.
(26) Jeong, S.; Park, J.; Pathania, D.; Castro, C. M.; Weissleder, R.; Lee, H. *ACS Nano* **2016**, *10* (2), 1802−1809.
(27) Staubach, S.; Razawi, H.; Hanisch, F. G. *Proteomics* **2009**, *9* (10), 2820−2835.
(28) Mei, Y.; Cai, D.; Dai, X. *J. Cancer* **2020**, *11* (5), 1162−1169.
(29) Osta, W. A.; Chen, Y.; Mikhitarian, K.; Mitas, M.; Salem, M.; Hannun, Y. A.; Cole, D. J.; Gillanders, W. E. *Cancer Res.* **2004**, *64* (16), 5818−5824.
(30) Li, J.; Liu, L.; Feng, Z.; Wang, X.; Huang, Y.; Dai, H.; Zhang, L.; Song, F.; Wang, D.; Zhang, P.; Ma, B.; Li, H.; Zheng, H.; Song, F.; Chen, K. *Breast Cancer* **2020**, DOI: 10.1007/s12282-020-01058-3.
(31) Ciravolo, V.; Huber, V.; Ghedini, G. C.; Venturelli, E.; Bianchi, F.; Campiglio, M.; Morelli, D.; Villa, A.; Mina, P. D.; Menard, S.; Filipazzi, P.; Rivoltini, L.; Tagliabue, E.; Pupa, S. M. *J. Cell. Physiol.* **2012**, *227* (2), 658−667.
(32) Rong, L.; Li, R.; Li, S.; Luo, R. *Oncol. Lett.* **2016**, *11* (1), 500−504.
(33) Grasso, L.; Wyss, R.; Weidenauer, L.; Thampi, A.; Demurtas, D.; Prudent, M.; Lion, N.; Vogel, H. *Anal. Bioanal. Chem.* **2015**, *407* (18), 5425−5432.
(34) Jiang, X. J.; Lau, J. T. F.; Wang, Q.; Ng, D. K. P.; Lo, P. H. *Chem. - Eur. J.* **2016**, *22* (24), 8273−8281.
(35) Takada, T.; Tochi, T.; Nakamura, M.; Yamana, K. *Bioorg. Med. Chem. Lett.* **2014**, *24* (12), 2661−2663.
(36) Maroto, R.; Zhao, Y.; Jamaluddin, M.; Popov, V. L.; Wang, H.; Kalubowilage, M.; Zhang, Y.; Luisi, Y.; Sun, H.; Culbertson, C. T.; Bossmann, S. H.; Motamedi, M.; Brasier, A. R. *J. Extracell. Vesicles* **2017**, *6* (1), 1359478.
(37) Dong, H.; Chen, H.; Jiang, J.; Zhang, H.; Cai, C.; Shen, Q. *Anal. Chem.* **2018**, *90* (7), 4507−4513.
(38) Alvarez-Erviti, L.; Seow, Y.; Schapira, A. H.; Gardiner, C.; Sargent, I. L.; Wood, M. J. A.; Cooper, J. M. *Neurobiol. Dis.* **2011**, *42* (3), 360−367.
(39) He, F.; Wang, J.; Yin, B. C.; Ye, B. C. *Anal. Chem.* **2018**, *90* (13), 8072−8079.
(40) You, M.; Yang, S.; Tang, W.; Zhang, F.; He, P. G. *ACS Appl. Mater. Interfaces* **2017**, *9* (16), 13855−13864.
(41) Wang, X.; Zhou, J.; Yun, W.; Xiao, S.; Chang, Z.; He, P.; Fang, Y. *Anal. Chim. Acta* **2007**, *598* (2), 242−248.
(42) Yang, S.; You, M.; Yang, L.; Zhang, F.; Wang, Q.; He, P. *J. Electroanal. Chem.* **2016**, *783*, 161−166.
(43) Wang, J.; Li, W.; Lu, Z.; Zhang, L.; Hu, Y.; Li, Q.; Du, W.; Feng, X.; Jia, H.; Liu, B. F. *Nanoscale* **2017**, *9* (40), 15598−15605.
(44) Wang, L.; Chen, G.; Zhao, J.; Cai, N. *J. Mol. Catal. B: Enzym.* **2016**, *133*, S468−S474.
(45) Dakova, I.; Vasileva, P.; Karadjova, I. *Bulg. Chem. Commun.* **2011**, *43* (2), 210−216.

https://dx.doi.org/10.1021/acs.analchem.0c00106
Anal. Chem. 2020, 92, 5404−5410